

# A Centrality and Spectral Framework for Enhancing SANReN Topology Resilience

Kerry-Lynn Whyte

whyker001@myuct.ac.za

Computer Science Department, University of Cape Town

## Abstract

The South African National Research and Education Network (SANReN) provides high-speed infrastructure for academic and research collaboration but faces limited last-mile connectivity and resilience to node failures. This project investigates whether node centrality metrics (measuring node criticality) and spectral metrics (capturing overall connectivity) can identify critical points of failure and inform resilience-oriented topology design. Experiments on three city-level SANReN topologies used a composite centrality measure to rank nodes and introduce redundancy. Spectral metrics (algebraic connectivity and eigenvalue multiplicity) of the current and redundant topologies were then assessed under node and edge removals. Redundant topologies generally showed higher resilience. NS-3 simulations of the Johannesburg topologies confirmed enhanced resilience under small-scale critical node failures. However, identical resilience was observed in the topologies under simulated edge failures. The results indicate that centrality metrics can accurately identify critical nodes and, together with spectral metrics, provide a framework for designing more resilient SANReN topologies.

## Keywords

NRENs; SANReN; network resilience; topological analysis; simulation; centrality; spectral metrics

## 1. Introduction

National Research and Education Networks (NRENs) are specialised internet providers that provide the support required for research and educational activities within a country as well as internationally [14, 16]. NRENs provide connectivity on a global scale through links to international RENs such as the UbuntuNetAlliance (Africa) and GÉANT (Europe) [16]. In addition, NRENs provide high-speed and widely available broadband connectivity to digital ecosystems which create economic development and income growth [17].

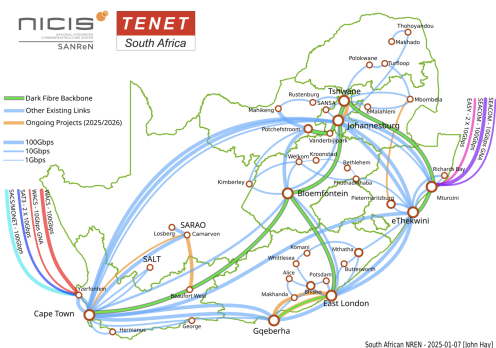


Figure 1: SANReN Network Backbone Diagram [32]

The South African NREN includes a backbone national fibre network with several high-speed 100Gbps links, smaller 10Gbps regional links, and connections from undersea cable stations located at Yzerfontein and Mtunzini [32]. SANReN also uses five undersea cables and several city-wide networks [32]. This backbone supports numerous high-data research applications in which high-speed, large-volume data transfers occur.

In 2018, SANReN implemented a pilot programme to upgrade the core backbone network capacity, implementing 10 Gbps data transfer nodes with the aim of improving transfer speeds and reliability when transmitting large datasets. The pilot results revealed a demand for a national infrastructure to support these large data transfers [29]. This demand is also due to SANReN's support of numerous data-intensive research applications, which require high speeds to transfer large volumes of data [29].

However, according to Bashir [3], SANReN's current network topology will face scalability challenges in the future due to newly available technologies and the 7.1% rise in the university gross enrollment ratio (GER) from 2021 to 2022 [11]. The increasing number of students at universities will increase bandwidth demand. Therefore, SANReN needs to 'future-proof' broadband availability to ensure this demand can be fulfilled [3]. Despite infrastructure improvements, such as the implementation of 100 Gbps data transfer nodes, congestion persists on key links. A study by Pillay et. al [29] found that similar data transfer speeds were observed from Johannesburg to Washington and to Cape Town, suggesting that local links are more saturated. These factors limit high-speed, low-latency research collaboration. Therefore, continued investment in improving resilience and performance in SANReN's topologies is required to enhance speed and ensure low-latency research collaboration.

Understanding which nodes are critical to a topology's connectivity and performance is key to designing resilient topologies. Centrality metrics quantify each node's relative importance, enabling the identification of critical nodes whose failure may compromise performance or disrupt connectivity. However, node-level centrality does not capture the global resilience of the network. To address this, spectral metrics, such as algebraic connectivity and eigenvalue multiplicity, measure overall resilience and connectivity of the network under failure scenarios. Cao et al. [5] found that redundancy—a process in which additional edges are added to a topology—can improve resilience. These perspectives motivate a dual analysis of SANReN's topology using both centrality and spectral metrics, leading to two core research questions:

### 1.1. Research Questions:

- (1) Can composite centrality scores (averaged from degree, betweenness, and closeness) correctly identify SANReN's known critical failure nodes?
- (2) To what extent can critical nodes – identified via centrality metrics – combined with spectral metric analysis, inform the redesign of resilience-oriented topologies?

This research investigates whether composite centrality scores – calculated by averaging degree, closeness, and betweenness centrality scores – can accurately identify known critical nodes within SANReN's city-level topologies. It further explores whether composite centrality scores, combined with spectral metric analysis, can guide the design of more resilient topologies. To evaluate this, redundant edges are added to the most critical nodes, and the spectral metrics of the current and redundant topologies are compared under node and edge removal experiments. Network simulations are also conducted on the Johannesburg topology to validate improvements in resilience when comparing the current and proposed redundant topologies. Analysing the spectral metrics, graph visualisations and the packet delivery ratios of the current and redundant SANReN topologies reveals the extent to which centrality and spectral metrics can inform the design of resilience-oriented topologies.

## 2. Background

### 2.1. Internet Topology

The logical level of a network topology consists of devices operating at the Internet Protocol layer [8]. The Internet Protocol layer determines how data is routed between nodes in the network. Logical topologies have been the focus of early research as they define the paths data takes through the network, irrespective of the physical connections [8]. The logical topology reveals routing dependencies, such as which nodes rely on one another to transmit data, and bottlenecks, where the network may become congested if certain nodes and paths are overloaded with traffic or fail [8]. Understanding the logical topology is critical for assessing reliability and resilience.

The physical topology refers to the physical infrastructure of the network, such as fibre-optic cables and switching devices [6]. The physical topology considers geographic constraints, physical distances, and infrastructure placement, which affect latency, redundancy, and vulnerability to failure [6]. Therefore, it is necessary to study network resilience.

### 2.2. Distance and Centrality metrics

2.2.1. *Distance metrics* are an example of traditional graph metrics that quantify the shortest path between two nodes in a graph [12]. Distance metrics such as network diameter, which measures the maximum distance of all shortest paths between pairs of nodes, are useful in assessing network resilience under node failures [castillo, 13].

2.2.2. *Centrality Metrics* identify critical nodes in a network, enabling the design of resilient networks [34]. Betweenness centrality measures how often a node occurs on shortest paths, highlighting key connector nodes which may fragment the network if they fail

[ghanbari, 18]. Closeness centrality measures how quickly a node can reach other nodes, reflecting a node's efficiency in spreading information or recovering from disruptions [28]. Degree centrality indicates the number of direct connections a node has to other nodes [28]. High-degree nodes often serve as hubs (nodes with a large number of direct connections to other nodes), which can cause network failure if they fail [30].

### 2.3. The Normalised Laplacian Matrix

The **Laplacian matrix** is a mathematical tool used to study the topological and resilience properties of networks. The normalised version adjusts for differences in node degrees, such that resilience comparisons can be drawn between networks of different sizes and connectivity patterns [10]. It is defined as:

$$L_{norm}(G)(i, j) = \begin{cases} 1, & \text{if } i = j \text{ and } d_i \neq 0 \\ -\frac{1}{\sqrt{d_i d_j}}, & \text{if } i \text{ and } j \text{ are connected} \\ 0, & \text{otherwise} \end{cases}$$

where  $d_i$  and  $d_j$  are the number of edges attached to each nodes  $i$  and  $j$  which are referred to as the degree of the nodes

2.3.1. *Eigenvalues* provide a mathematical method of quantifying network connectivity and resilience. Let  $M$  be a symmetric matrix and  $I$  the identity matrix of order  $n$ . Eigenvalues are the roots of the characteristic polynomial:

$$\det(M - \lambda I) = 0$$

For Laplacian matrices, eigenvalues lie in the range  $[0, 2]$ .

### 2.4. Spectral Metrics

Spectral metrics provide a quantitative measure of global network resilience. They are derived from the eigenvalues of the Laplacian matrix.

2.4.1. *Eigenvalue Multiplicity* indicates the number of disconnected components in the network and is represented by the count of zero eigenvalues in the Laplacian spectrum. A single zero indicates a fully connected network. Multiple zeros indicate network fragmentation and low resilience. Therefore, monitoring changes in multiplicity after simulated critical node and edge failures reveals whether redundant topologies improve resilience based on whether they fragment less than the current topologies.

2.4.2. *Algebraic Connectivity*,  $a(G)$ , more sensitively and broadly captures the connectivity of graphs than average node degree [23].  $a(G)$  is the second smallest eigenvalue of the Laplacian spectrum,  $\lambda_2$  [24]. A higher  $a(G)$  indicates a more resilient network with higher fault tolerance, while a smaller  $a(G)$  reflects lower resilience and a higher risk of network fragmentation under node failures [10].

2.4.3. *The Spectral Model*: applies spectral metrics to the Laplacian matrix to evaluate global network resilience in node and edge failure scenarios such that resilient topologies can be designed [33, 6].

## 2.5. Graph Models

Graph models visualise the topology. Gabriel graphs define connections based on node proximity [6], effectively capturing grid-like physical structures, but failing to capture star-like logical topologies [6]. The Kamada Kawai algorithm [21] is useful for graph visualisations as it obtains the geometric distances between vertices, which are similar to the underlying graph distances [21]. Therefore, Kamada Kawai graphs correlate with actual network layouts as they preserve graph-theoretic distances, supporting more accurate visual assessments across diverse topology sizes and structures.

## 2.6. Network Simulation

Network simulation utilises mathematical models to represent network component and protocol behaviour [22]. By executing discrete events over simulated time, it allows researchers to test networks and determine their resilience under failures, and congestion [19]. Simulation supports repeatable and controlled experimentation by enabling researchers to vary network conditions and parameters [19].

**NS-3** is an open-source simulation software providing scalability and stress-testing of topological models [26, 20]. Events are executed sequentially in simulated time, allowing researchers to test network behaviour under various conditions in a repeatable and modular manner.

**The packet delivery ratio** indicates the reliability of the network. It measures the percentage of packets successfully received at the destination in comparison to the number of packets initially sent by the source node.

## 3. Related Work

Previous analyses of NRENs have highlighted the value and limitations that topological evaluation provides.

### 3.1. Physical and Logical Topologies

Studies by Çetinkaya et al. [10, 7] and Lee et al. [23] found that physical network topologies often follow transport corridors, which are critical points of vulnerability for SANReN. However, modelling physical topologies is costly and therefore, resilience improvements are budget-constrained [9]. Logical topologies are a cost-effective alternative. However, their frequently star-like structures, which concentrate traffic through high centrality nodes, introduce single points of failure [10]. Therefore, modelling SANReN's logical layer is essential for understanding how node failures affect resilience.

In terms of SANReN-specific work, Salie [31] observed large delays in SANReN topologies such as Cape Town. However, the study lacks spectral and centrality metrics, simulation as well as graph visualisations to support its claims.

### 3.2. Analysing Topologies

**3.2.1. Traditional graph metrics** such as centrality metrics, identify structural weaknesses in the topology but fail to capture the structural differences and temporal variations of dynamic topologies

[4]. In addition, these metrics are also not suitable when comparing graphs of different sizes [10]. However, as SANReN expands its topologies to accommodate growing research and connectivity demands, comparisons between topologies of different sizes and configurations will become necessary, and traditional graph metrics may obscure resilience improvements.

Çetinkaya et. al's [10] comparison of the centrality metrics of physical and logical topologies revealed that physical topologies distribute connectivity more evenly, while logical topologies depend on highly connected central nodes. For SANReN, reliance on key connector nodes in logical topologies may expose the network to vulnerabilities if those nodes fail. Whereas a more balanced physical topology could improve resilience. However, due to the connectivity differences in physical and logical topologies network resilience should not be assessed on centrality metrics in isolation.

Distance metrics such as network diameter also indicate resilience. However, Çetinkaya et. al [10] found that physical topologies had a larger network diameter than logical topologies. Therefore, assessing resilience based on distance metrics in isolation may result in resilience conclusions that misrepresent the physical topology.

**3.2.2. Spectral metrics** have become the focus of research to evaluate resilience. Alenazi et. al [17] found that logical topologies have higher algebraic connectivity than physical topologies and are thus, more resilient [10, 7]. Thus, creating a logical topology with higher algebraic connectivity is critical in ensuring that the physical topology is also resilient [24]. However, algebraic connectivity cannot be used to compare graphs of different orders as larger graphs exhibit lower connectivity values as they are larger and more complex [10]. Since SANReN's topology will expand with demand, algebraic connectivity alone is not a reliable indicator of network connectivity.

### 3.3. Simulation for validation

Simulation tools like NS-3 provide controlled environments to test and reproduce resilience indicator metrics such as the packet delivery ratio, despite scalability and obsolescence challenges [19]. Experimental research has demonstrated NS-3's ability to produce realistic models. For example, Mezzavilla et al. [25] utilised NS-3 to provide an efficient link performance metric, and Alberro et al. [1] simulated data centre environments with NS-3. A study by Egho-Promise et. al [15] found that topologies with higher packet delivery ratios showed greater resilience, confirming packet delivery ratios are an effective resilience indicator. NS-3 remains unused for assessing the resilience of SANReN. However, NS-3 can validate the resilience improvements indicated by spectral metrics through packet delivery ratio analysis under simulated stress-testing of the current and proposed topologies after each node and edge removal increment.

## 4. Experimental Design and Implementation:

The experiments are designed to assess the extent to which critical nodes (identified by centrality metrics), in combination with spectral metrics, can inform the redesign of resilience-oriented topologies, under critical node and edge failures. Four experiments were

conducted on each of SANReN's city-level topologies. Firstly, the *edge addition experiment* added additional edges to critical nodes in the current topologies, creating redundant topologies. The *critical node removal* and *critical-node-based edge removal* experiments, designed to simulate node and edge failures, then assessed the spectral metrics (eigenvalue multiplicity and algebraic connectivity) of the current and redundant topologies under incremental critical node and critical-node-based edge removals. Improved spectral resilience in the redundant topologies would indicate the effectiveness of the spectral and centrality metric-driven redesign. As a further validation step, the fourth experiment involved an NS-3 simulation of the Johannesburg topology, where the current and proposed topologies' packet delivery ratios were compared under large data loads. If the proposed redundant topology had higher packet delivery ratios, which indicates increased resilience, then this further validates the spectral metric analysis suggesting enhanced resilience in the redundant topologies.

## 4.1. Metrics

**4.1.1. Spectral and Centrality metrics** provide complementary measures of network resilience. Spectral metrics, derived from the eigenvalues of the graph Laplacian, such as algebraic connectivity and eigenvalue multiplicity quantify global connectivity and redundancy properties. In contrast, centrality metrics such as degree, closeness, and betweenness centrality assess the relative importance of individual nodes such that critical nodes can be identified.

In order to compute spectral metrics, the NetworkX [27] Python package is utilised to construct, manipulate and analyse the structure of complex networks [27]. NetworkX converts the graph into a normalised Laplacian matrix. The centrality metrics (closeness, degree, and betweenness) can then be derived from this matrix using NetworkX's built-in functions. Spectral and centrality metrics were computed using a Python script (Metrics.py). Spectral metrics computed by this script included algebraic connectivity and eigenvalue multiplicity, while centrality metrics included degree, closeness, and betweenness centrality. For spectral metrics, the Laplacian matrix is converted into a dense matrix using NumPy. This conversion enables computation of eigenvalues. The spectral metrics are then defined from these eigenvalues, where algebraic connectivity is the second smallest eigenvalue in the matrix ( $\lambda_2$ ), and eigenvalue multiplicity ( $m_0$ ), is the count of zero eigenvalues in the matrix.

**4.1.2. Packet Delivery Ratio (PDR)** To obtain the packet delivery ratio in NS-3, the FlowMonitor is triggered to analyse collected data and mark lost packets. A map is stored of flow statistics - one entry per each flowID's communication flow. For each flow, *tx* counts the number of transmitted packets and *rx* counts how many of the transmitted packets were successfully received. All the flows' *txPackets* and *rxPackets* are then added together to get *totalTx* and *totalRx*. The packet delivery ratio is then computed by:

$$PDR = \left( \frac{\text{totalRx}}{\text{totalTX}} \right) \times \frac{1}{100}$$

## 4.2. Datasets

**4.2.1. tgf files** contain information regarding SANReN city-level topologies. They are formatted as a list of name and their corresponding numbers. This is followed by a series of lines containing all the links, e.g., (1 2) is an edge between node 1 and 2. The tgf files used included 3 different-sized city-level topologies: Cape Town (cpt.tgf) - a large topology containing 69 nodes and 99 edges, as well as Johannesburg (jnb.tgf) - a medium sized topology containing 32 nodes and 60 edges. In addition, Pietermaritzburg (pzb.tgf) - a smaller topology containing 11 nodes and 13 edges was used. The experiments were conducted on these 3 topologies to evaluate whether centrality metrics can successfully identify SANReN's critical failure nodes, and whether combining these with spectral metrics enhances resilience across topologies of varying sizes.

**4.2.2. isis-links.json**, is a file containing information regarding each link as well as its maximum bandwidth. This file is utilised to map the nodes in .tgf files to their corresponding speeds (e.g., 100Mbps) by storing the speeds associated with each network link and then looking up the corresponding speeds when loading in the links from the .tgf files to be stored in a graph CSV file. If the speed is unknown, no speed mapping exists for the link, and speed is defaulted to 100 Mbps.

## 4.3. Software

Visual Studio Code was utilised as the project space. Metrics were computed using NetworkX in conjunction with NumPy to calculate the spectral and centrality metrics for each experiment. The outputted topology and metric files are in a CSV format. Matplotlib was utilised to plot spectral metrics, graph visualisations, and the NS-3 packet delivery ratios.

## 4.4. Methods

**4.4.1. Reading in and storing graphs:** SANReN tgf files were parsed in, and their corresponding bandwidths were obtained from the link mapping JSON file. The topology details were written to a CSV file in the format: Source, Destination, Bandwidth, Delay. Source, Destination, and Bandwidth are determined from the mapping, but delay is derived from the bandwidth due to the absence of precise link distance data. Delays were approximated using fixed values derived from link bandwidths. This approach is based on the inverse relationship between bandwidth and transmission delay, expressed as  $D_T = \frac{N}{R}$ , where  $N$  is the packet size and  $R$  the link bandwidth [2]. For instance, 100 Mbps links were assigned 10 ms delays, while 10 Gbps links were given 2 ms delays.

**4.4.2. Spectral Metric computation:** For spectral metrics, Network X converts the topology graph into a normalised Laplacian matrix, which is then converted into a dense matrix using NumPy. This conversion allows computation of eigenvalues. The spectral metrics are then defined from these eigenvalues, where algebraic connectivity,  $a(G)$ , is represented by the second smallest eigenvalue ( $\lambda_2$ ), and eigenvalue multiplicity ( $m_0$ ) is the count of zero eigenvalues.

**Algorithm 1** Spectral Metrics Calculation

---

**Input:** Graph  $G$   
**Output:** Algebraic connectivity and zero multiplicity

```

Compute Laplacian matrix  $L$  of  $G$ 
Compute eigenvalues of  $L$  and sort in ascending order
 $a(G) \leftarrow$  second-smallest eigenvalue (or 0 if  $|V| < 2$ )
 $m_0 \leftarrow$  number of eigenvalues equal to 0
return  $a(G), m_0$ 
```

---

**4.4.3. Centrality metric ranking computation:** The centrality metric ranking algorithm identifies and ranks critical nodes in each topology based on their importance. This algorithm is essential to verify the extent to which centrality metrics can identify vulnerable nodes, and informs the critical node and edge removal experiments. For the rankings to be computed, the topology is loaded from a CSV file. The degree, betweenness, and closeness centrality metrics are then obtained using NetworkX. Since centrality metrics output values on different scales, they are normalised in the range  $[0, 1]$ , and a composite average is calculated for each node. The nodes are then ranked from most to least critical and exported to two CSV files. One file contains node IDs (used to inform node and edge removal experiments), and another file contains node IDs with their names (used for validation). SANReN network engineers confirmed the algorithm was correctly ranking and identifying critical nodes for each city-level topology.

**Algorithm 2** Composite Centrality Ranking

---

**Input:** Graph  $G$   
**Output:** Sorted list of composite centrality ranked nodes

```

Compute degree, betweenness, and closeness centralities of  $G$ 
Normalize each centrality measure to the range  $[0, 1]$ :
  for each centrality score  $c$  do
     $c_{\text{norm}}(v) \leftarrow \frac{c(v) - \min(c)}{\max(c) - \min(c)}$ 
  for each node  $v \in V(G)$  do
    Compute composite score:
     $\text{score}(v) \leftarrow \frac{\deg_{\text{norm}}(v) + \text{bet}_{\text{norm}}(v) + \text{close}_{\text{norm}}(v)}{3}$ 
Sort nodes by composite score in descending order
return sorted node list and scores
```

---

**4.4.4. Simple topology operations:** The framework also enables targeted removal and addition of individual nodes or edges. This extension is useful if SANReN needs to monitor how network resilience is affected by targeted node and edge removals in the future.

**4.5. Ethics and Limitations:**

No ethical concerns occurred, as the topological data used was obtained from SANReN with permission for resilience analysis. While a redundancy addition experiment enhanced the redundancy of critical nodes, the pre-removal resilience results obtained by the experiment were excluded from resilience validation as the study focused on resilience under critical node and edge failures.

**4.6. Experiments**

The node and edge removal experiments were conducted on each city's current and proposed (redundant) topology. The redundant topology was obtained using the edge addition experiment - which incrementally added edges to the most critical nodes. The topologies' algebraic connectivity and eigenvalue multiplicity responses to the removal of critical nodes and critical-node-based edge removals were then plotted as line graphs, revealing the extent to which spectral and centrality metrics can be utilised to propose more resilient topologies. If the proposed topologies' spectral metrics indicate improved resilience, then the metrics can be concluded as successful at proposing more resilient topologies.

**4.6.1. Edge addition (redundancy enhancement)** To assess whether spectral and centrality metrics can inform the design of more resilient proposed topologies, a critical-node-based edge addition experiment was conducted. This algorithm incrementally introduces redundant edges by targeting the most critical nodes, as determined by the precomputed centrality ranking. This method adds redundant edges to the top 1, 2, 5 and 10 most critical nodes cumulatively. A copy of the original graph is made such that the original graph is unchanged. The current metrics are then computed and stored before any edges are added. For each increment level  $n$ , the top- $n$  critical nodes are identified. For each of these nodes, it then finds nodes to which it is not yet connected to and selects the top 2 most central non-neighbours (based on the same centrality ranking). Edges are then added between the current node and these two candidate nodes.

**Algorithm 3** Edge Addition for Redundancy Enhancement

---

**Input:** Graph  $G$ , Centrality ranking list  $R$ , Increment set  $I = \{1, 2, 5, 10\}$   
**Output:** Updated graph  $G_{\text{redundant}}$  and dictionary of metrics

```

Make a copy of the original graph  $G \rightarrow G_{\text{redundant}}$ 
Compute and store current metrics:
 $M_0 \leftarrow \text{compute\_and\_return\_metrics}(G_{\text{redundant}})$ 
  for each  $n \in I$  do
    Let  $T \leftarrow$  top- $n$  most critical nodes from  $R$ 
    for each  $v \in T$  do
      Let  $N_v \leftarrow$  current neighbours of  $v$  in  $G_{\text{redundant}}$ 
      Let  $U \leftarrow$  nodes not in  $N_v$  and not equal to  $v$ 
      Sort  $U$  by centrality rank in  $R$ 
      Let  $U_{\text{top}2} \leftarrow$  first 2 nodes in sorted  $U$ 
      for each  $u \in U_{\text{top}2}$  do
        if  $(v, u) \notin E(G_{\text{redundant}})$  then
          Add edge  $(v, u)$  to  $G_{\text{redundant}}$ 
Compute and store updated metrics:
 $M_n \leftarrow \text{compute\_and\_return\_metrics}(G_{\text{redundant}})$ 
return  $G_{\text{redundant}}, \{M_n\}$ 
```

---

**4.6.2. Critical Node Removal Experiment** This experiment is designed to compare the spectral metric responses of the current

and proposed (redundant) city-level topologies under critical node removals to determine the overall change in resilience when redundancy is added. This enables the evaluation of whether critical nodes identified by centrality metrics, combined with spectral metrics, can inform the redesign of more resilient topologies under critical node failures. A ranked node centrality text file is loaded, and based on the centrality rankings, critical nodes are then removed in increments from the top 1 to 10 most critical nodes from the current and proposed topologies. This experiment is deterministic as the nodes removed are removed based on the pre-computed centrality ranking text file. The spectral metrics for both topologies for each increment are then recorded in separate CSV files and plotted as line graph comparative visualisations of the proposed and current topologies' spectral metric responses to the various node removal increments. The line graphs show the resilience trend in the current versus the proposed topologies. Kamada-Kawai graph visualisations are iteratively generated after each removal step to provide visual resilience validation.

---

**Algorithm 4** Critical Node Removal Experiment
 

---

**Input:** Current topology  $G_{init}$ , Redundant topology  $G_{red}$ , Ranked node list  $R$   
**Output:** Spectral metrics recorded after removals ( $a(G)$  and  $m_0$ ) for each topology and spectral metric plots

```

Load ranked node list R
for each  $k$  in removal increments  $\{1, 2, \dots, 10\}$  do
     $R_k \leftarrow$  top- $k$  critical nodes from  $R$ 
     $G_{init}^k \leftarrow$  copy of  $G_{init}$  with nodes in  $R_k$  removed
     $G_{red}^k \leftarrow$  copy of  $G_{red}$  with nodes in  $R_k$  removed
    Compute Laplacian  $L_{init}^k$  and  $L_{red}^k$ 
    Compute eigenvalues for  $L_{init}^k$  and  $L_{red}^k$ 
     $a_{init}^k \leftarrow$  second-smallest eigenvalue of  $L_{init}^k$ 
     $m_{init}^k \leftarrow$  number of eigenvalues equal to 0 in  $L_{init}^k$ 
     $a_{red}^k \leftarrow$  second-smallest eigenvalue of  $L_{red}^k$ 
     $m_{red}^k \leftarrow$  number of eigenvalues equal to 0 in  $L_{red}^k$ 
    Save spectral metrics of both topologies to CSV files
    Visualise  $G_{init}^k$  and  $G_{red}^k$ ;
  Plot and save  $a(G)$  and  $m_0$  responses across removals for both topologies
return Spectral metrics across all increments for both topologies
  
```

---

**4.6.3. Critical-Node-Based Edge Removal Experiment** This experiment is designed to compare the spectral metrics of the current and proposed (redundant) city-level topologies under incremental edge removals from a fixed, most critical node. This enables the evaluation of whether critical nodes identified by centrality metrics, together with spectral metrics, can inform the redesign of more resilient topologies under critical edge failures. The most critical node is identified using a pre-computed centrality ranking based on the current (non-redundant) topology. This ensures that both topologies are subjected to identical failure scenarios, allowing for controlled comparison. For each edge removal step (0%, 25%, 50%,

and 75%), a copy of the base topology (before any edge removals) is used to ensure non-cumulative and independent edge removals. A list of the node's incident edges is extracted using NetworkX's `G.edges(node)` function. This function returns the edges in a consistent order based on the graph's internal structure. The script then iterates over the list, removing edges in percentage increments from the most critical node. The edge removal procedure is deterministic as it relies on precomputed node rankings of the current topology, consistent edge ordering, and consistent edge removal selection logic. This guarantees that identical input topologies produce identical edge removal sequences and spectral metric outcomes, ensuring reproducible evaluation of network resilience under targeted edge failures at the most critical node. After each removal step, spectral metrics are computed for both the current and proposed topologies. The metrics are saved and visualised as line graphs to assess whether centrality and spectral metrics jointly improve resilience in the current and redundant topologies under edge removal.

---

**Algorithm 5** Critical-node-based Edge Removal Experiment
 

---

**Input:** Current topology  $G_{init}$ , Redundant topology  $G_{red}$ , Ranked node list  $R$   
**Output:** Spectral metrics after incremental edge removals from the most critical and spectral metric plots

```

Load ranked node list R
 $N_c \leftarrow$  top-ranked (most critical) node from  $R$ 
 $E_c \leftarrow$  incident edges of  $N_c$  in  $G$ , with duplicate undirected edges removed
for each  $p$  in removal percentages (0%, 25%, 50%, 75%) do
     $k \leftarrow \lfloor p \times |E_c| \rfloor$ 
     $E_{remove} \leftarrow$  first  $k$  edges in  $E_c$ 
     $G_{init}^p \leftarrow$  fresh copy of  $G_{init}$ 
     $G_{red}^p \leftarrow$  fresh copy of  $G_{red}$ 
    Remove  $E_{remove}$  from  $G_{init}^p$  and  $G_{red}^p$ 
    Compute Laplacians  $L_{init}^p$ ,  $L_{red}^p$ 
    Compute eigenvalues for  $L_{init}^p$ ,  $L_{red}^p$ 
     $a_{init}^p \leftarrow$  second-smallest eigenvalue of  $L_{init}^p$ 
     $m_{init}^p \leftarrow$  number of eigenvalues equal to 0 in  $L_{init}^p$ 
     $a_{red}^p \leftarrow$  second-smallest eigenvalue of  $L_{red}^p$ 
     $m_{red}^p \leftarrow$  number of eigenvalues equal to 0 in  $L_{red}^p$ 
  Save spectral metrics of both topologies to respective CSV files
  Plot and save  $a(G)$  and  $m_0$  responses across removals for both topologies
return Spectral metrics for all removal levels across both topologies
  
```

---

**4.6.4. NS-3 Resilience Validation** The NS-3 simulation script aims to validate the resilience conclusions regarding the extent to which spectral metrics can propose the redesign of more resilient topologies. This script automates performance testing on Johannesburg's current and redundant topologies by processing the topology files

generated after each critical node removal step and critical-node-based edge removal increment. For each topology, it builds the network in NS-3, simulates traffic between nodes using UDP echo, and then records performance metrics such as the Packet Delivery Ratio using FlowMonitor. The resulting packet delivery ratios of the current and proposed (redundancy-enhanced) topologies are then plotted such that resilience comparisons can be drawn.

## 5. Results and Discussion

### 5.1. Critical Node Removal Experiment:

The first experiment compares the spectral metrics of the current and proposed (redundant) city-level topologies under critical node removals to evaluate whether critical nodes identified by centrality metrics, together with spectral metrics, can inform the redesign of more resilient topologies under critical node failures.

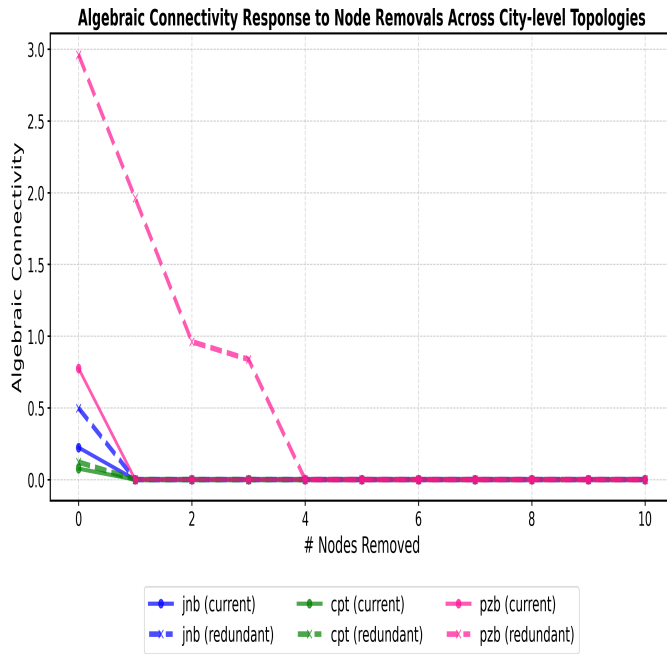
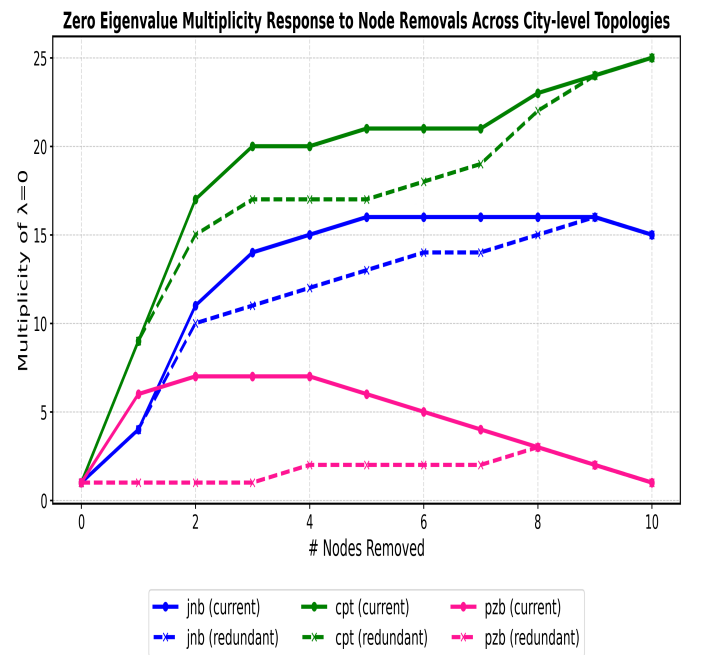


**Figure 2: Comparison of Algebraic Connectivity Responses to Top 1–10 Critical Node Removals in Initial vs. Redundant City-Level Topologies**

Figure 2 illustrates that for Pietermaritzburg, the proposed (redundant) topology's algebraic connectivity was higher than the current topology's up until 3 critical nodes were removed. However, algebraic connectivity converged to 0 in the redundant topology after removing the top 4 most critical nodes, indicating that the graph was no longer connected. However, this is due to the Pietermaritzburg topology containing only 11 nodes and thus, removing 4 critical nodes fragmented the network (see Figure 10 in the appendix as evidence). Therefore, when removing a larger number of critical nodes in smaller topologies, connectivity is still lost despite the added redundancy in the proposed topology.

Figure 2 illustrates that Johannesburg and Cape Town's redundant

topologies also exhibited higher algebraic connectivity before node removals due to the added redundancy. This redundancy increases connectivity and resilience. However, in both cities, the algebraic connectivity of the redundant topologies dropped to 0, converging with the current topology, after the most critical node was removed. This suggests the node functioned as a hub, playing a key bridging role that the redundant links failed to compensate for when the critical node failed.



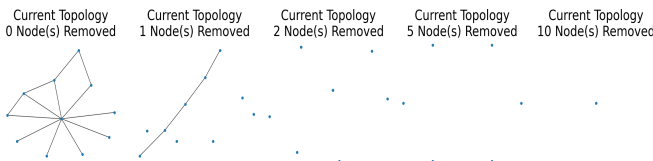
**Figure 3: Comparison of Zero Eigenvalue Multiplicity Responses to Top 1–10 Critical Node Removals in Initial vs. Redundant City-Level Topologies**

Figure 3 illustrates that for all node removal increments in the Pietermaritzburg topology, the redundant topology generally exhibited a lower and more stable multiplicity than the current topology. In the current topology, multiplicity initially increased until 4 critical nodes were removed. This is likely because the removed critical nodes connected subgraphs such that their removal caused fragmentation. However, subsequent removals affected low-centrality, isolated nodes that didn't contribute to further fragmentation, so multiplicity gradually decreased in the current topology. After 8 node removals, the redundant topology converged with the current topology. This is explained by the topology's small size of 11 nodes and 13 edges. Therefore, after 8 removals, only 3 disconnected nodes remained, resulting in a multiplicity of 3.

However, Figure 3 illustrates that for Johannesburg and Cape Town, the redundant topologies consistently exhibited a lower multiplicity than the current topologies for all critical node removal increments greater than 1. This suggests that the added redundancy provides alternative paths under node failures, preventing fragmentation and

enhancing resilience. However, in both cities, the multiplicity of the redundant and current topologies was equal when only the most critical node was removed. This is because the edge addition reinforced paths between multiple high-centrality nodes, so removing one node did not disrupt the topology enough to cause fragmentation. However, as the removal increments increased beyond just 1 node removal, the redundant topologies' resilience benefits are observed as they fragmented less than the current topologies.

All the topologies' multiplicities converged after removing the 10 most critical nodes. This is likely due to the redundancy strategy focusing on the top 10 most critical nodes, such that redundancy was not evenly distributed throughout the topology. In Pietermaritzburg, this convergence resulted in a multiplicity of 1, as due to the small topology size, 10 removals left only a single remaining node. In contrast, Johannesburg and Cape Town's multiplicities converged to 15 and 25, indicating greater fragmentation. This suggests that while redundancy can initially lower the multiplicity and therefore, fragmentation observed as a result of node removals, the enhanced resilience provided by redundancy diminishes when redundant links are not evenly distributed throughout the topology. Finally, the resilience was further validated through graph visualisations after each removal increment.



**Figure 4: Pietermaritzburg Current (initial) Topology After Critical Node Removal Steps**

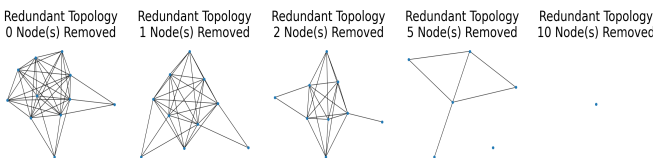


**Figure 5: Pietermaritzburg Redundant Topology After Critical Node Removal Steps**

Figure 4 and 5 depict Pietermaritzburg's current and redundant topologies after removal of the top 1,2,5, and 10 most critical nodes. The current topology (Figure 4) fragmented significantly after just two node removals, while the redundant topology (Figure 5) remains well-connected even after 10 removals, demonstrating greater resilience. Similar trends were observed across all three cities. Full visualisations of each removal increment are provided in the appendix. For Pietermaritzburg, see Figures 11 and 12; for Johannesburg, see Figures 13 and 14; and for Cape Town, see Figures 15 and 16.

## 5.2. Critical-Node-Based Edge Removal Experiment:

The second experiment compares the spectral metrics of the current and proposed (redundant) city-level topologies under critical-node-based edge removals to evaluate whether spectral and centrality metrics can inform the redesign of more resilient topologies under critical edge failures.

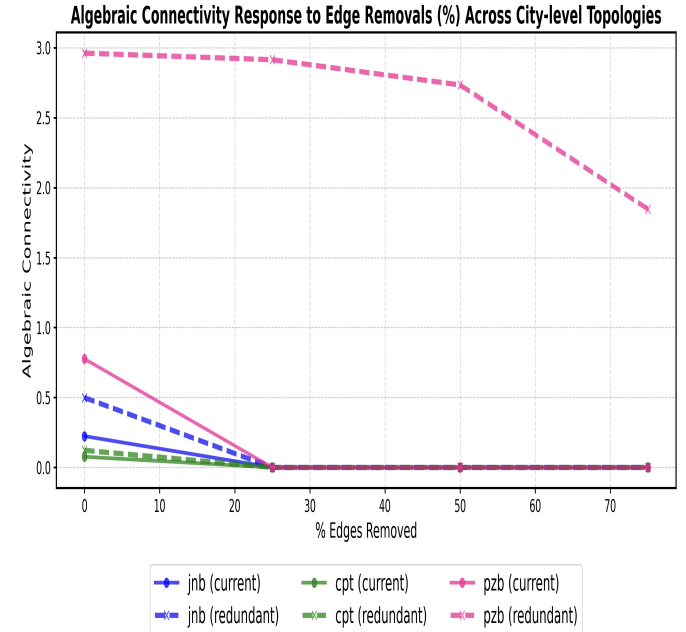


**Figure 6: Algebraic Connectivity Responses to Edge Removal Increments of 25%, 50% and 75% from the Most Critical Node in Current and Redundant Topologies**

Figure 6 illustrates that for the Pietermaritzburg topology, the algebraic connectivity was consistently higher for the redundant topology across all edge removal increments due to the added edges between critical nodes. Even after 75% of edges were removed, the redundant topology maintained higher connectivity than the initial topology before any edge removals, implying greater resilience in the redundant topology. The decrease in the algebraic connectivity was more gradual in the redundant topology than in the initial topology, indicating that it loses connectivity at a slower rate.

Figure 6 illustrates that for the larger Johannesburg and Cape Town topologies, the redundant topologies also exhibited higher algebraic connectivity than the current topologies before edge removals. However, after 25% of edges were removed from the most critical node, both topologies exhibited an equal connectivity of 0. The redundant topologies experienced a sharper decline, under edge removals than the current topologies. This steeper drop is due to the edge addition strategy, which increases the number of edges incident to the critical node such that when a fixed percentage of edges were removed, more edges were removed from the redundant topology.

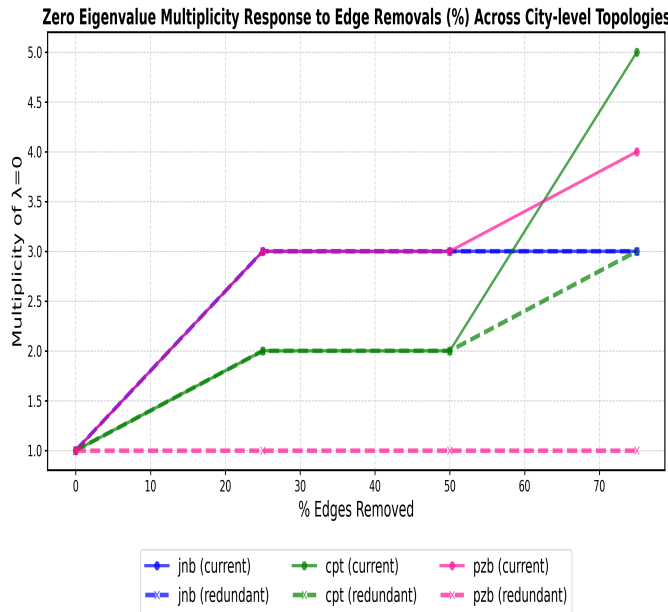


**Figure 7: Zero Eigenvalue Multiplicity Responses to Edge Removal Increments of 25%, 50% and 75% from the Most Critical Node in Current and Redundant Topologies**

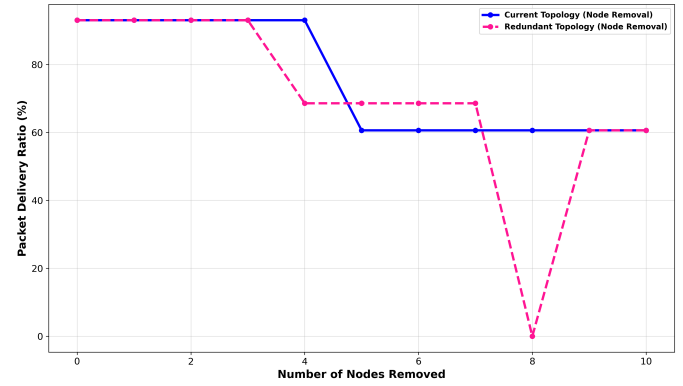
In terms of eigenvalue multiplicity, Figure 7 illustrates that in the Pietermaritzburg topology, the current topology's multiplicity exhibited an increasing trend as more edges were removed from the most critical node, indicating fragmentation. In contrast, the redundant topology exhibited a constant multiplicity of 1 across all edge removal increments. Therefore, the redundant topology remained connected and exhibited greater resilience than the current topology.

Figure 7 illustrates that Johannesburg's topologies exhibited equal multiplicity values across all removal increments. This is due to the redundancy strategy adding edges to the top 10 critical nodes, while edge removals only targeted the most critical node. Despite a larger number of edges being removed from the redundant graph (due to its higher initial edge count), eigenvalue multiplicity remained stable, since redundancy was distributed across the other high-criticality nodes. This suggests neither of the topologies fragmented.

Similarly, Figure 7 illustrates that Cape Town exhibited identical eigenvalue multiplicities in both its topologies across edge removal increments of up to 50%, indicating no improvement in resilience. However, at 75% edge removal, the current topology's multiplicity increased to 5, indicating 5 disconnected components, whereas the redundant topology had a multiplicity of 3. This suggests that the redundant topology fragmented less and was more resilient under larger edge removal increments. This is likely due to the redundant graph's additional edges, which provided alternative paths for maintaining connectivity.

### 5.3. NS-3 Resilience Validation

The third experiment compares the packet delivery ratio (which is higher in more resilient topologies) of Johannesburg's current topology with its proposed redundant topology under both node and edge removal experiments as validation of the spectral and centrality metrics' ability to inform the redesign of resilient topologies.



**Figure 8: Packet Delivery Ratios of Current vs. Redundant Johannesburg Topologies After Removal of the Top 1–10 Most Critical Nodes**

Figure 8 shows both topologies maintained stable packet delivery ratios of 93% up to 4 node removals. At 4 removals, the redundant topology's ratio dropped to 68%, while the current topology remained stable at 93%, indicating improved resilience due to the alternate paths provided by redundancy. From 4 to 5 removals, the current topology dropped to 61%, whereas the redundant topology plateaued at 68%. However, at 8 removals, the redundant topology collapsed to 0% as redundancy was concentrated around the top 10 high-centrality nodes. Once these were removed, the network lost all viable paths. In contrast, the current topology retained partial connectivity through fewer central nodes. Although the redundant packet delivery ratio recovered slightly at 9 removals, it remained lower than earlier levels, suggesting limited resilience. These results indicate that redundancy provided short-term resilience, but as more critical nodes were removed, resilience diminished.

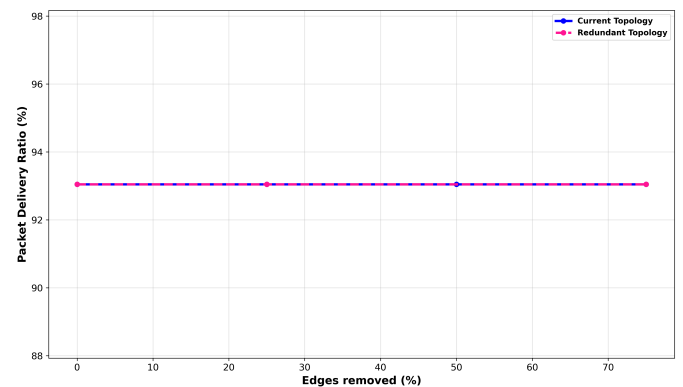


**Figure 9: Packet Delivery Ratios of Current vs. Redundant Johannesburg Topologies After Edge Removals of 25%, 50%, and 75% from the Most Critical Node**

Figure 9 illustrates that under all edge removal scenarios, Johannesburg's current and redundant topologies' packet delivery ratios remained stable. This suggests that the current Johannesburg topology exhibits strong resilience to edge failures. Although redundancy did not enhance the packet delivery ratio, it also did not diminish it, confirming the resilience of the proposed redundant design under extensive edge failures.

#### 5.4. Discussion

The node removal experiment revealed that for smaller topologies, the proposed (redundant) topologies had a significantly lower and more stable multiplicity, suggesting less fragmentation and therefore, enhanced resilience. The exception occurred when critical node removals resulted in a graph consisting of a single node, as this resulted in both topologies being fully connected. However, in larger topologies, the reduction in multiplicity was only observed after critical node removals greater than one. For example, the multiplicity of the redundant and proposed Johannesburg and Cape Town topologies remained the same when the most critical node was removed, demonstrating that redundancy has a greater impact on resilience under larger critical node removal increments. The algebraic connectivity of all three cities' topologies decreased after removing the most critical node due to the star-like centrality of the most critical node, which resulted in fragmentation despite added redundancy. This supports Cetinkaya et al.'s claim [10] that algebraic connectivity alone is insufficient to measure topology resilience.

The edge removal experiment illustrated that the redundancy in the proposed topologies improves network resilience overall. In smaller topologies, added redundancy prevented fragmentation after edge removals, resulting in lower multiplicity in redundant topologies than in the current topologies. However, in Johannesburg, the redundant and current topologies exhibited equal resilience under all edge removal increments. This occurred because the edge removal targeted the most critical node, which had more edges in the redundant topology due to the additional edges added by redundancy. This resulted in more edges being removed from the redundant topology, cancelling out the resilience benefit. In larger topologies such as Cape Town, resilience improvements emerged only at high removal thresholds (75%), where alternative paths from redundant links became critical to maintaining connectivity.

The NS-3 simulation experiments reinforced these findings. Under node removals, both topologies maintained a 93% packet delivery ratio up to 4 removals. At 4 removals, the redundant topology degraded to 68% while the current topology remained stable. Between 4 and 5 removals, the current topology dropped to 61%, whereas redundancy preserved a higher level of connectivity (68%). However, at 8 removals, the redundant topology's packet delivery ratio dropped to 0% due to redundancy being concentrated around the top 10 most critical nodes before rising again after 9 and 10. In contrast, the current topology retained stable connectivity via fewer central nodes. These findings validate the resilience-enhancing potential of redundant links in the short-run, but suggest that redundancy must be distributed across the network to provide long-term resilience

under node failures. However, under edge removals, both topologies maintained a stable 93% packet delivery ratio, indicating high resilience. Therefore, under edge-based failures, NS-3 simulation did not provide additional evidence to validate or refute the spectral metric-based resilience analysis of topologies.

These findings address the research questions as the consistent impact of removing the highest-ranked nodes confirms that the composite centrality scores were effective in identifying SANReN's critical nodes. In addition, the comparative analysis of multiplicity, algebraic connectivity, and NS-3 simulation results shows that combining centrality with spectral metrics can inform the redesign of resilience-oriented topologies, though the degree of improvement varies depending on topology size and the distribution of redundancy.

#### 6. Conclusion

This study demonstrates that composite centrality scores, derived from degree, betweenness, and closeness centrality, can correctly identify SANReN's critical failure nodes. SANReN network engineers confirmed that the centrality ranking algorithm consistently identified and ranked critical nodes in all three city-level topologies. Moreover, the consistent degradation in resilience following the removal of top-ranked nodes supports the validity of the composite ranking approach. These centrality-based rankings informed where redundancy was introduced in the proposed topologies.

The results further show that critical nodes identified via centrality metrics, when combined with spectral metric analysis, can guide the redesign of resilience-oriented topologies. For smaller topologies like Pietermaritzburg, the proposed (redundant) topologies exhibited higher resilience under critical node and edge removals with lower eigenvalue multiplicity and higher initial algebraic connectivity before any removals. However, in larger topologies such as Cape Town, redundant topologies were more resilient under critical node failures and larger edge removal increments. Johannesburg presented mixed results as redundancy improved resilience under node removals but had no effect on resilience under edge removals. Therefore, for redundancy to meaningfully improve edge-level resilience, it must be both strategically placed and not concentrated only at the nodes most likely to be compromised.

While the algebraic connectivity in all the city-level topologies was higher before removals (due to the redundant edges added), it dropped after the most critical node was removed and after 25% edge removal, reinforcing that algebraic connectivity cannot be analysed in isolation to assess network resilience.

The graph visualisations of redundant and current topologies indicated that redundant topologies were more connected under critical node failures than the current topologies.

NS-3 simulation of the Johannesburg topology confirmed that redundancy extended the topology's ability to sustain high packet delivery ratios under smaller critical node removal increments. However, the results also showed that the redundant topology exhibited reduced resilience at 4 removals, and completely collapsed

at 8. Meanwhile, the current topology retained partial stability through fewer central nodes. The packet delivery ratios under the critical edge removal experiment indicate that the topologies were equally resilient in simulation, suggesting that redundancy did not reduce resilience, even if spectral metrics showed varying resilience indications in redundant topologies. These findings underline the resilience-enhancing potential of redundancy, but highlight that redundancy must be distributed across the network to provide sustainable resilience under extensive node failures.

Therefore, these findings demonstrate that composite centrality scores can effectively identify critical nodes, which can then be utilised in combination with spectral metrics to inform the redesign of resilience-oriented topologies by observing spectral metrics under node and edge removals in the current and proposed (redundant) topologies. Thus, offering a framework for informing the redesign of SANReN's topologies to enhance resilience. However, for redundant redesigns to yield sustained resilience benefits, redundancy must be distributed across the topology rather than concentrated solely at the most central nodes.

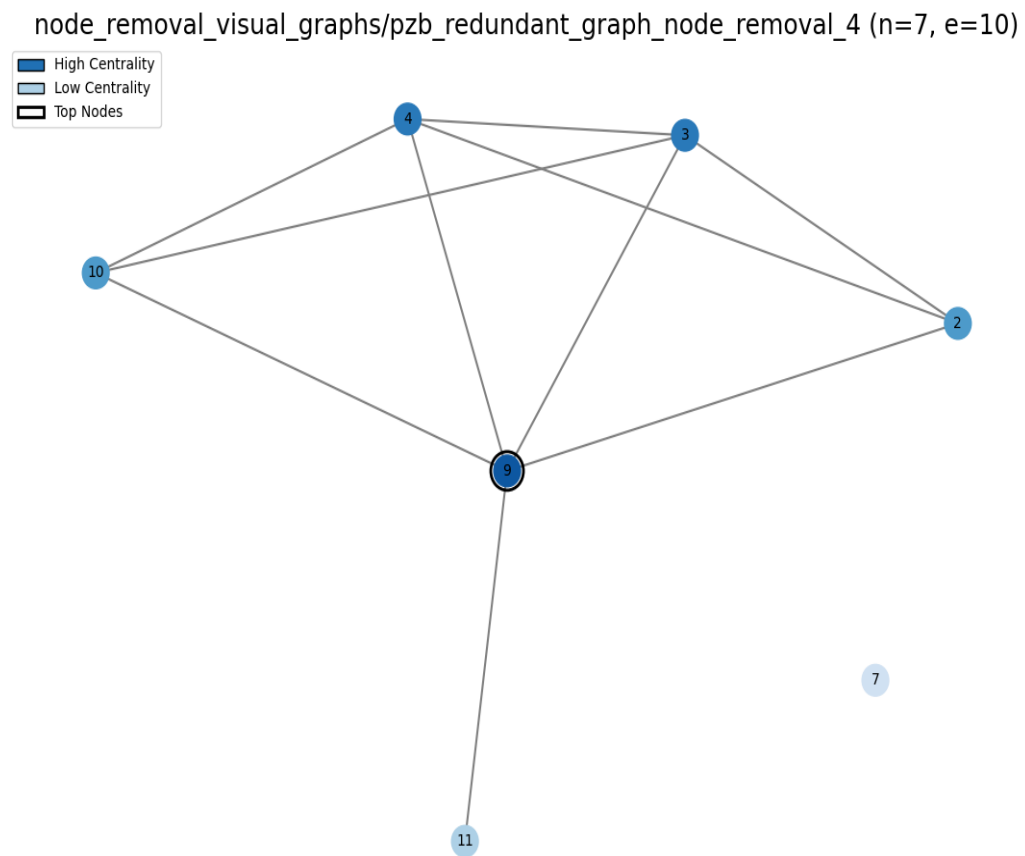
## 7. Future work

Future work can extend the analysis to SANReN's other city-level topologies to evaluate if similar resilience patterns emerge, and the resilience can also be validated using NS-3 simulations. Future work can focus on random critical node and critical-node-based edge removals and these experiments could be repeated to ensure reliable results. Additionally, instead of concentrating redundancy at high-centrality nodes, future work can test distributed redundancy strategies to assess their effect on resilience using spectral and NS-3 metrics. Finally, simulation of attack scenarios can be performed in NS-3 using dynamic traffic models to enable a more realistic validation of network resilience.

## References

- [1] Leonardo Alberro, Felipe Velázquez, Sara Azpiroz, Eduardo Grampin, and Matías Richart. 2022. Experimenting with routing protocols in the data center: an ns-3 simulation approach. *Future internet*, 14, (Oct. 2022), 292–292. doi: 10.3390/fi14100292.
- [2] Baeldung. 2021. Propagation delay vs transmission delay, (Mar. 2021). Retrieved Sept. 6, 2025 from <https://www.baeldung.com/cs/propagation-vs-transmission-delay>.
- [3] Sajitha Bashir. 2020. Connecting africa's universities to affordable high-speed broadband internet: what will it take? World Bank, (Dec. 2020). Retrieved Mar. 19, 2025 from <https://openknowledge.worldbank.org/entities/publication/c9dc3411-3b35-55b0-a6ba-da8b91d1fa90>.
- [4] Ghanshyam S. Bopche and Babu M. Mehtre. 2017. Graph similarity metrics for assessing temporal changes in attack surface of dynamic networks. *Computers Security*, 64, 16–43. doi: <https://doi.org/10.1016/j.cose.2016.09.010>.
- [5] Xian-Bin Cao, Chen Hong, Wenbo Du, and Jun Zhang. 2013. Improving the network robustness against cascading failures by adding links. *Chaos, Solitons Fractals*, 57, (Dec. 2013), 35–40. doi: 10.1016/j.chaos.2013.08.007.
- [6] Egemen K. Çetinkaya, Mohammed J.F. Alenazi, Yufei Cheng, Andrew M. Peck, and James P.G. Sterbenz. 2014. A comparative analysis of geometric graph models for modelling backbone networks. *Optical Switching and Networking*, 14, (June 2014), 95–106. doi: 10.1016/j.osn.2014.05.001.
- [7] Egemen K. Çetinkaya, Mohammed J. F. Alenazi, Andrew M. Peck, Justin P. Rohrer, and James P. G. Sterbenz. 2015. Multilevel resilience analysis of transportation and communication networks. *Telecommunication Systems*, 60, (Mar. 2015), 515–537. doi: 10.1007/s11235-015-9991-y.
- [8] Egemen K. Çetinkaya, Mohammed J.F. Alenazi, and James P.G. Sterbenz. 2013. Network design and optimisation based on cost and algebraic connectivity. *2013 5th International Congress on Ultra Modern Telecommunications and Control Systems and Workshops (ICUMT)*, 14, 193–200. doi: 10.1109/ICUMT.2013.6798426.
- [9] Egemen K. Çetinkaya, Mohammed J.F. Alenazi, Yufei Cheng, Andrew M. Peck, and James P.G. Sterbenz. 2013. On the fitness of geographic graph generators for modelling physical level topologies. *2013 5th International Congress on Ultra Modern Telecommunications and Control Systems and Workshops (ICUMT)*, 14, 38–45. doi: 10.1109/ICUMT.2013.6798402..
- [10] Egemen K. Çetinkaya, Mohammed J.F. Alenazi, Justin P. Rohrer, and James P.G. Sterbenz. 2012. Topology connectivity analysis of internet infrastructure using graph spectra. *2012 IV International Congress on Ultra Modern Telecommunications and Control Systems*, (Oct. 2012). doi: 10.1109/icumt.2012.6459764.
- [11] Natalie Cowling. 2024. South africa: gross tertiary school enrollment ratio. Statista. (Nov. 2024). Retrieved Mar. 27, 2025 from <https://www.statista.com/statistics/1261626/south-africa-gross-tertiary-school-enrollment-ratio/>.
- [12] Kenneth Dadedzi. 2014. *The Distance Matrix of a Graph*. Master's thesis. Stellenbosch University, (May 2014), 1.
- [13] Anthony Dekker and Bernard Colbert. 2004. Network robustness and graph topology. *Australasian Computer Science Conference*, 26, (Feb. 2004).
- [14] John Dyer. 2009. The case for national research and education networks (nrens). (2009). Retrieved Mar. 16, 2025 from <https://casenornrens.org/wp-content/uploads/2021/05/Case-for-NRENs.pdf>.
- [15] Ehigitor Egho-Promise, Zeeshan Pervez, Hewa Balisane, George Asante, Folayo Aina, and Halima Kure. 2025. Optimizing secure routing protocols for resilience network communications. *International Journal of Research - GRANTHAALAYAH*, 13, (June 2025), 51–69. doi: 10.29121/granthaalayah.v13.i6.2025.6221.
- [16] Michael Foley. 2016. The role and status of national research and education networks (nrens) in africa. World Bank Group, (June 2016). Retrieved Mar. 11, 2025 from <https://documents.worldbank.org/en/publication/documents-report/s/documentdetail/233231488314835003/the-role-and-status-of-national-research-and-education-networks-nrens-in-africa>.
- [17] Broadband Commission for Sustainable Development. 2015. The state of broadband: broadband as a foundation for sustainable development. (Sept. 2015).
- [18] Linton C. Freeman. 1977. A set of measures of centrality based on betweenness. *Sociometry*, 40, 1, 35–41.
- [19] Jose Gomez, Elie F. Kfouri, Jorge Crichigno, and Gautam Srivastava. 2023. A survey on network simulators, emulators, and testbeds used for research and education. *Computer Networks*, 237, (Dec. 2023), 1–42. doi: 10.1016/j.comnet.2023.110054.
- [20] Thomas R Henderson, Mathieu Lacage, and George F Riley. 2008. Network simulations with the ns-3 simulator. (Aug. 2008). Retrieved Mar. 19, 2025 from <http://conferences.sigcomm.org/sigcomm/2008/papers/p527-hendersonA.pdf>.
- [21] Tomihisa Kamada and Satoru Kawai. 1989. An algorithm for drawing general undirected graphs. *Information Processing Letters*, 31, 1, 7–15. doi: [https://doi.org/10.1016/0020-0190\(89\)90102-6](https://doi.org/10.1016/0020-0190(89)90102-6).
- [22] James F. Kurose and Keith W. Ross. 2017. *Computer Networking: A Top-Down Approach*. (7th ed.). Pearson, Boston, MA.
- [23] Hyeongjik Lee, Seonkoo Jeong, and Kwanghee Lee. 2023. The south korean case of deploying rural broadband via fiber networks by implementing universal service obligation and public-private partnership based project. *Telecommunications Policy*, 47, 3, 102506. doi: <https://doi.org/10.1016/j.telpol.2023.102506>.
- [24] William Liu, Harsha Sirisena, Krzysztof Pawlikowski, and Allan McInnes. 2009. Utility of algebraic connectivity metric in topology design of survivable networks. *UC Research Repository (University of Canterbury)*, 4, (Oct. 2009), 131–138. doi: 10.1109/drcn.2009.5340016.
- [25] Marco Mezzavilla, Marco Miozzo, Michele Rossi, Nicola Baldo, and Michele Zorzi. 2012. A lightweight and accurate link abstraction model for the simulation of lte networks in ns-3. *CiteSeer X (The Pennsylvania State University)*, (Oct. 2012), 55–60. doi: 10.1145/2387238.2387250.
- [26] Network Simulator Network and Mobility. 2025. Ns-3. Network Simulator Network and Mobility. (2025). Retrieved June 9, 2025 from <https://www.nsnam.org>.
- [27] NetworkX. 2025. Networkx network analysis in python. NetworkX.org. (Aug. 18, 2025). <https://networkx.org>.
- [28] Mark Newman. 2010. *Networks: An Introduction*. Oxford University Press.
- [29] Kasandra Pillay, Johann Hugo, Thuso Bogopa, Manqoba Shabalala, Thokozani Khwela, and Ajay Makani. 2024. Sanren's 100 gbps data transfer services transferring data fast! (Nov. 2024), 765–769. doi: 10.1109/scw63240.2024.00109.
- [30] Ravi Ramesh. n.d. Centrality measures for networks (part 6). [https://www.albany.edu/~ravi/pdfs/part\\_06.pdf](https://www.albany.edu/~ravi/pdfs/part_06.pdf). Lecture slides, CSI 445/660, University at Albany. (n.d.). Retrieved Sept. 5, 2025 from.
- [31] Luqmaan Salie and Josiah Chavula. 2021. Measuring sanren performance: an internal and external view - uct computer science research document archive. Proceedings of Southern Africa Telecommunication Networks and Applications Conference (SATNAC), (2021). doi: [https://pubs.cs.uct.ac.za/id/eprint/1524/1/35\\_Final\\_Paper.pdf](https://pubs.cs.uct.ac.za/id/eprint/1524/1/35_Final_Paper.pdf).
- [32] SANReN. 2025. South african nren backbone – sanren. SANReN, (2025). Retrieved Mar. 27, 2025 from <https://www.sanren.ac.za/backbone/>.

- [33] Tristan A. Shatto and Egemen K. Çetinkaya. 2017. Variations in graph energy: a measure for network resilience. *2017 9th International Workshop on Resilient Networks Design and Modeling (RNDM)*, 1–7. doi: 10.1109/RNDM.2017.8093019.
- [34] Zelin Wan, Yash Mahajan, Beom Kang, Terrence Moore, and Jin-Hee Cho. 2021. A survey on centrality metrics and their network resilience analysis. *IEEE Access*, PP, (July 2021), 1–1. doi: 10.1109/ACCESS.2021.3094196.

**Appendix A – Pietermaritzburg Redundant Topology After Removing the Top 4 Most Critical Nodes****Figure 10: Pietermaritzburg Redundant Topology After Removing the Top 4 Most Critical Nodes**

## Appendix B – Pietermaritzburg Node Removal Experiment Graphs



**Figure 11: Pietermaritzburg's Current Topology After Critical Node Removals**

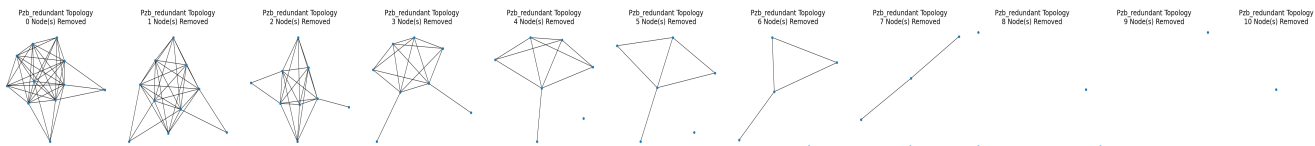


**Figure 12: Pietermaritzburg's Redundant Topology After Critical Node Removals**

## Appendix C – Johannesburg Node Removal Experiment Graphs

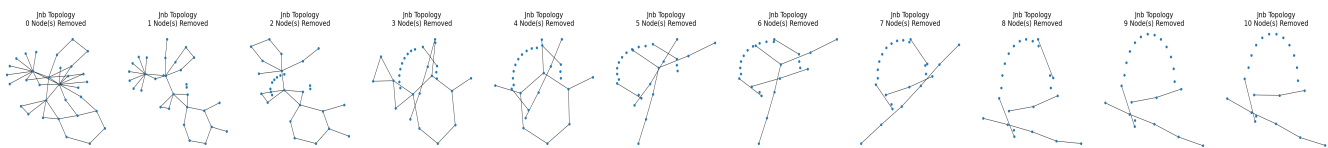


**Figure 13: Johannesburg's Current Topology After Critical Node Removals**

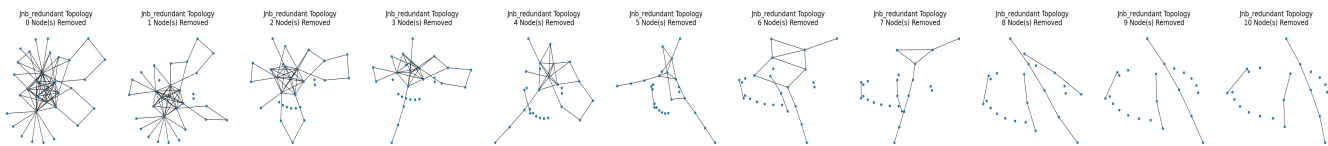


**Figure 14: Johannesburg's Redundant Topology After Critical Node Removals**

## Appendix D – Cape Town Node Removal Experiment Graphs

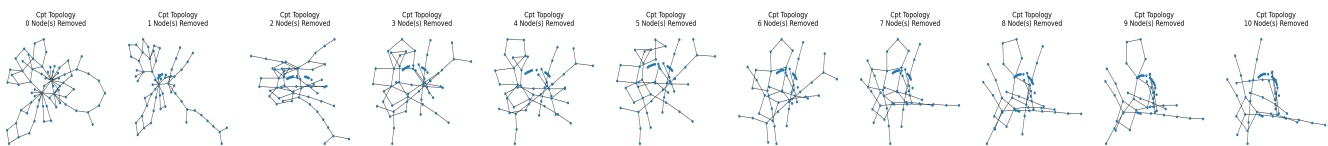


**Figure 15: Cape Town's Current Topology After Critical Node Removals**

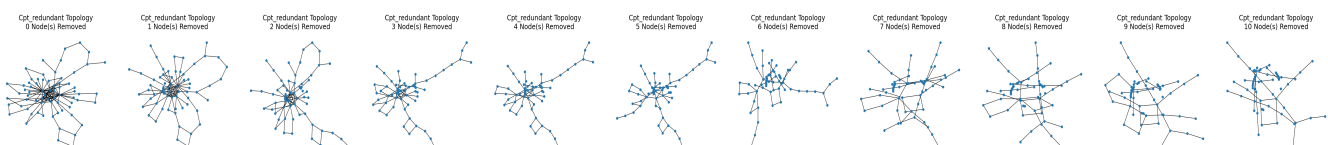


**Figure 16: Cape Town's Redundant Topology After Critical Node Removals**